

# Incorporating fire severity for refined data-drive carbon emissions estimates of boreal and temperate forest fires in the Generic Carbon Budget Model (GCBM)

[ ]<sup>1</sup>, <sup>2</sup>, <sup>3</sup>, <sup>1</sup>, <sup>3</sup>, and <sup>3</sup>

<sup>1</sup>  
<sup>2</sup>  
<sup>3</sup>

**Correspondence:** ()

**Abstract.** Wildfire is the most impactful natural disturbance to Canada's boreal and temperate forest biomes. Current representations of fire impact on forest carbon stocks is limited to a single parameterization of fire severity (i.e. the fraction of biomass consumed) that assumes only high severity fires, despite a large and increasing evidence base of widespread mixed-severity wildfire. In this submodel of the larger Generic Carbon Budget Model for forest carbon accounting, field measurements of biomass consumption as related to satellite-derived burn severity maps are interpreted from a fire physics and ecology perspective to derive algorithms to describe forest carbon fluxes in the immediate aftermath of fires. Model outputs indicate total carbon emissions range from a 11 t C/ha in Boreal Shield West forests of Saskatchewan following low severity fire to over 70 t C/ha in Taiga Cordillera and Pacific Maritime forests of Yukon under high severity fire. Pacific Maritime forest showed the largest fraction of carbon release in the canopy biomass pools (67%), while Taiga Shield West and Boreal Plains of the Northwest Territories and Manitoba were estimated of having 82% of carbon emissions in the surface and belowground biomass pools of litter, duff, peat, roots, etc.

. His Majesty the King in Right of Canada as represented by the Minister of Natural Resources Canada. This work is distributed under the Creative Commons Attribution 4.0 License.

## 1 Introduction

Wildfire is on par with insects as the largest stand-replacing disturbance process in Canada's forest, impacting ~1-3 Mha of Canada's 355 Mha forested area in a typical year (Hanes et al., 2019). In Canada's reliable 53-year burned area record, nine years have exceeded 4 Mha of burned area (or approximately 1% of Canada's forest area) (Skakun et al., 2022). The 2023 fire season in Canada burned a remarkable 15 Mha owing to extreme drought, severe fire weather conditions, and a prolonged fire season length (Jain et al., 2024).

20 Of this, managed forest accounts for xxx% of the area burned between 1972 and 2024; publicly-owned managed forest under long-term licence to private timber companies forms 40% of Canada's forest area (Stinson et al., 2019). Privately-owned forest constituting only 6% of the forest area, with the remainder of the forest area being a mix of formally protected areas, remote unmanaged forest, Indigenous reserve lands and other uses without large-scale harvesting. Managed forest areas adjacent to communities have historically shown some local fire suppression effects with a bias towards older forest nearby boreal forest  
25 communities in Canada (Parisien et al., 2020), though the effect is limited to a 25 km radius between these widely dispersed communities.

Burned area is dominated by a relatively small number of very large fires, with 3% of fires constituting 97% of the burned area (Stocks et al., 2002). Lightning-caused fires account for approximately half of all ignitions and between xxx and xxxx% of burned area, but no distinction is made between human and lightning ignition for carbon accounting purposes. Annual  
30 burned area mapping at 30 metre resolution is conducted using a composite of satellite and aerial mapping; the relatively small number of large fires, and their slow vegetation regeneration (White et al., 2017) allows for reliable mapping using multispectral imagery such as Landsat within one year of the fire (Whitman et al., 2018).

In CBM-CFS, spatially referenced stand lists representing large homogenous stands that fall within spatial units (ecozone-provincial intersections) are randomly (??) drawn (Kurz et al., 2002), even when applying precisely mapped burned areas  
35 (Hall et al., 2020). CBM-CFS currently assesses (simulates?, calculates?) fire impacts to carbon pools only as representing high-severity fire, which is the most common of three severity classes of burned forest in Canada (Hall et al., 2008). Biomass consumption estimates are based on the and the assumption of complete crown mortality, with additional biomass consumption following a spatially-referenced aggregated estimate at the ecozone-province of annualized drought conditions.

In Canada's forests, a combination of disturbance history, soils, and less frequently topographic variables determine leading  
40 tree species; at local scales (1-100 ha), tree species plays a major role in determining ecosystem susceptibility to fire (Bernier et al., 2016) where older, conifer-dominated forests burn at very high rates relative to adjacent deciduous or mixed stands. Even when deciduous and mixed forests do burn, they do so at consistently lower severity compared to all but the most xeric conifer forests (Whitman et al., 2018). Thus, important biases in fire activity towards older and moderate to poorly-drained forests are not resolved, and only a regionally-averaged fire severity is applied.

45 To support recent advances in operational burn severity mapping for Canada (Whitman et al., 2020) alongside multi-decade reliable burned area records that provide certainty on fire start and end dates (Hall et al., 2020) , the CBM DMs also need to be upgraded.

something about dynamic veg models like landis and how they represent fire disturbance -then how most MRV models and quickly how they do fire disturbance -even a bit on the GFED/GFAS world too

50 that ESSD frames it well, worth reading the intro part in detail) (recent Smyth and Campbell papers too) (other recent Canadian fire-carbon things, Walker - esp is supports consistent patterns in proportional carbon loss)

In this document, we outline the evidence-based fire Disturbance Matrices updated and designed for a spatially-explicit update to the CBM, anchored in a three severity class paradigm. These fire carbon flux models are built from a blend of aggregated field data linked to remotely sensed severity, as well as insights from fire physics and experimental fires. Key

55 knowledge gaps are also highlighted, with interim solutions presented until further quantification can be done in field studies, such as from further wildfire observations, experimental fires, or prescribed fires.

## 2 Methods

### 2.1 Carbon Modeling Spatial Units

- show RU map twice, with softwood foliage and then BGSlow pool size as colour ramp on two maps?

### 60 2.2 Biomass pools of the Generic Carbon Budget Model

Short section explaining the pool definitions most relevant to fire.

### 2.3 Axioms of forest carbon budget after fire

To simplify the process of the creation of the DMs as a distillation of the complexities of fire severity and combustion patterns, the following logical axioms are proposed and maintained throughout:

65 1. Disturbance matrices are to be in terms of mortality, not survival

2. Crown Fraction Burned (CFB) is a mass-based estimate of the portion of foliage consumed in the flaming passage of a fire, and is inclusive of merchantable and submerchantable trees, both broadleaf and needleleaf. Needles that are heat-killed but otherwise not consumed in the fire are not considered part of CFB, and are instead considered part of the foliage to litter biomass transfer.

70 3. The heat-killed but unconsumed fraction of the canopy is equal to (mortality - CFB)

4. In submerchantable trees, mortality = CFB

5. In submerchantable trees, mortality is  $\leq 1$

6. In merchantable trees, CFB  $\leq$  mortality

7. Snags are inclusive of both those killed by prior fire as well as those killed by all other causes

75 Of these, Crown Fraction Burned (CFB) is an important concept used primarily in fire behaviour science but not carbon accounting nor fire ecology. CFB was introduced in the 1992 Fire Behaviour Prediction System documentation (Group, 1992), and provides a simple continuous 0-100 variable for only the consumption of foliage (inclusive of both conifer and broadleaf), as opposed to ordinal and less precise systems like Crown Fire Severity Index that allows the user to specify which pools of canopy biomass are consumed, but not the degree to which a given pool is consumed.

**Table 1.** Emissions factors in flaming and smouldering phase, expressed as portion of unburned biomass carbon content

Spp	Flaming	Smouldering
CO2	0.868	0.703
CO	0.070	0.161
PM10	0.022	0.048
NMOG	0.016	0.035
PM25	0.019	0.040
CH4	0.005	0.013
BC	0.000	0.000

## 80    2.4   Ground plot and remotely sensed fire severity data

!!!Ellen to insert methods here - including the figure of where the samples are from etc.

## 2.5   Combustion gas emission ratios

Certain variables, like the partitioning of CO<sub>2</sub>:CH<sub>4</sub>:CO gas emissions, are constant throughout ecozones, but vary by flaming vs smouldering combustion modes. They are defined in a global variables table:

85    where CO<sub>2</sub> is responsible for 86.8% of emissions in the flaming phase, but only 70.3% of emissions in the smouldering phase, with a doubling of CO emissions and tripling of CH<sub>4</sub> emissions. With a Global Warming Potential of CO equal to 1.9 and CH<sub>4</sub> of 25, the Global Warming Potential per unit of biomass consumption in the smouldering phase is 1.18 times higher in global warming potential compared to flaming, not including differential aerosol production and injection heights, however. Note that these proposed emissions factors for flaming vs smouldering are aligned with those currently used in Canada's  
90    operational wildfire smoke air quality model, FireWork (Chen et al., 2019). With flaming and smouldering each contributing roughly equally to wildfire emissions, these distinct flaming and smouldering emissions rates correspond well with aircraft smoke chemistry observations by (Simpson et al., 2011) and (Hayden et al., 2022) and are themselves very similar to prior emissions factors used in CBM. Note that as current described, the sum of CO<sub>2</sub>, CH<sub>4</sub>, and CO emissions from wildfires only represent approximately 95% of the fire carbon mass emitted to the atmosphere, with 0.5-2.0% of biomass emitted as particulate  
95    matter (e.g. PM2.5, but also PM1 and PM10 classes of particulates at 1 and 10 um diameters, respectively), and an additional 3% (Hayden et al., 2022) to as little as 1% (Simon et al., 2010) composed of non-methane organic gases that have a large range in global warming potentials as compared to CH<sub>4</sub>.

## 2.6   Litter layer area-wise consumption by severity class

The litter layer forms the first biomass pool in which a spreading fire consumes fuel. In low-severity fires, the litter layer may

100   be consumed little to no underlying duff material consumed, nor any tree mortality (Hessburg et al., 2019). Logically, since

**Table 2.** Unburned litter area by ecozone and severity class. The majority of the data comes from studies in the Boreal Plains and Boreal Shield West, and so values are extrapolated from those two well-observed ecozones to all others.

Ecozone	Low	Mod	High
BSW	0.20	0.08	0.05
TP	0.14	0.16	0.03
TSW	0.20	0.08	0.05
BP	0.14	0.06	0.02
BC	0.14	0.06	0.02
BSE	0.20	0.08	0.05
TSE	0.20	0.08	0.05
MC	0.14	0.06	0.02
HP	0.20	0.08	0.05
TC	0.14	0.06	0.02
PM	0.14	0.06	0.02
AM	0.14	0.06	0.02
MP	0.14	0.06	0.02
P	0.14	0.06	0.02

litter consumption is required for the ignition of the underlying duff layer, this litter area-wise fractional consumption also informs and constrains duff consumption.

## 2.7 Duff Consumption

While consumption of fine fuels in the litter layer of the forest floor is nearly complete for any given fire intensity, consumption of deeper organic soil horizons (F+H layers in upland forests and upper peat layers in wetlands) is more drought dependent. In the fire literature in Canada, the soil organic layer is termed Forest Floor Fuel Load (FFFL) and is dominated by the equivalent Belowground Slow pool (BGSlow) in CBM. Typically attention has been paid to the absolute value of Forest Floor Fuel Consumption (FFFC); however in the case of carbon modelling, it is the relative fraction of consumption (FFFC/FFFL) that is of interest. In this scheme, we utilize a composite of wildfire data from (de Groot et al., 2009) alongside the ABoVE duff consumption data , with an alternative modelling approach to compute the relative amount of depth of consumption (scalar from 0 to 1) rather than an absolute value in  $\text{kg m}^{-2}$  or cm as otherwise done in the literature. A logit transform is used on the scalar data to make it suitable for the fitted non-linear least-squares modelling:

$$\text{logit} \left( \frac{\text{depthofburn}}{\text{prefiredepth}} \right) = [3.83(1 - e^{(-0.005DC)})] + (-0.718\log_e(\text{BGSlow})) \quad (1)$$

where DC is the Fire Weather Index Drought Code, and BGSlow in the CBM (given in Mg C/ha in this equation), and also

115 synonymous with the the Forest Floor Fuel Load (with ecozone averages given in (Letang and de Groot, 2012) or site-level data where observed). The modelling of relative depth of burn had a higher skill than modelling of the relative mass of consumption, given natural variability in soil density with depth.

A conversion factor is then applied to the relative depth of burn data to convert it to a relative mass consumption value. Since organic soil density always increases with depth, this conversion factor from depth to mass is less than one:

120 
$$\left( \frac{\text{massconsumed}}{\text{prefiremass}} \right) = \left( \frac{\text{depthofburn}}{\text{prefiredepth}} \right) * CF \quad (2)$$

where the Correction Factor is defined for boreal spruce fuel types as:

$$CF_{\text{spruce}} = 1.018(\text{RelativeDepth})^{0.250} \quad (3)$$

and for all other fuels as

$$CF_{\text{nonspruce}} = 0.13(\text{RelativeDepth}) + 0.87 \quad (4)$$

125 with RelativeDepth as a value from 0-1.

While ultimately this scheme can be used on individual fires with estimated or measured fuel loading and specific Drought Code values, for the purposes of this first assessment, an ecozone-averaged fuel load and decadal composites of Drought Code can also be used to provide representative values. Specifically, a median Drought Code of detected fire hotspots in Canada from 2003-2021 (Barber et al.) using the same data as the Canadian CFEEPS-FireWork wildfire air quality model of (Chen et al.,  
130 2019) is presented below, along with proportional consumption values of the forest floor by ecozone:

Note that the maximum upland Forest Floor Fuel Load is approximately 30 kg m-2 (Letang and de Groot, 2012); higher values are typically seen only in peat ecosystems, where the above scheme does not apply at a local scale since the fuel load (pool size) in peatlands is much larger, but absolute consumption values are similar between deep forest floor organic layers and peatlands (Walker). For Canadian peatlands, the CaMP model (Bona et al., 2020) is instead used in CBM. Within  
135 CaMP, a separate peatland water model driven by Drought Code determines the thickness of the unsaturated peat layer, and an amount approximating 12% of the thickness of the unsaturated peat is consumed as smouldering consumption. The peat-specific carbon pools and fire Disturbance Matrices are fully described in (Bona et al., 2020); large peatland trees will still utilize the DM scheme described below. Since deeper forest organic soil and peat layers show approximately similar absolute consumption rates, for the purpose of this general model description no peatland-specific components of the fire DMs are  
140 required.

Limited data is available on the fraction of woody debris consumption alongside fire severity measurements. Coarse woody debris of overstory stems that makes up 60-80% of woody debris biomass in Canada's boreal and temperate forests (Hanes

**Table 3.** Fire Weather, fuel loading, and duff consumption values per ecozone

Ecozone	Median Drought Code of Burning	Median FFFL kg m-2	FFFC kg m-2	% consumption
BSW	239	8.8	3.7	0.42
TP	369	15	7.01	0.47
TSW	297	1.7	1.33	0.78
BP	242	9.8	3.96	0.4
BC	250	8.31	3.72	0.45
BSE	123	10.9	1.95	0.18
TSE	98	1.7	0.71	0.42
MC	452	6	4.15	0.69
HP	204	7.9	3.02	0.38
TC	254	8.31	3.77	0.45
PM	268	15.2	5.45	0.36
AM	270	10.9	4.62	0.42
P	242	9.8	3.96	0.4

et al., 2021), with its moisture and consumption patterns largely follows the moisture regime of the Drought Code (McAlpine, 1995). In this modelling framework, the proportion of coarse (>7.5 cm diameter) and medium (>0.5 cm and <7.5 cm) woody

145 debris consumption is estimated based on detailed measurements of consumption from experimental fires. Coarse Woody Debris is responsible for approximately 50-75% of the total woody debris load in most ecozones, and approximately 60% of the total woody debris consumption. Ecozone-level CWD consumption rates are summarized as:

Note that where historical burn severity data is not available, and instead the fire classification type of surface, intermittent crowning, and active crown fire are used as proxies for low, moderate, and high severity fire, respectively. Fine woody debris 150 <0.5 cm in diameter is consumed at the exact same rate as the litter pool (see section above).

## 2.8 Drivers of C losses in the tree canopy

### 2.8.1 Overstory tree mortality and consumption

Numerous process-driven (Michaletz and Johnson, 2006) or empirical (Hood and Lutes, 2017) tree mortality models are present and show significant skill in predicting tree mortality based on fire behaviour (i.e. flame length, rate of spread). Since the 155 driving data in this model is satellite-derived fire severity over the landscape scale, fire behaviour metrics such as flame length or scorching height of bark are not available as a continuous mapped product. Instead, softwood and hardwood overstory mortality is calculated per ecozone as a function of satellite-observed fire severity using aggregated ground plot data:

And since large-diameter, live trees killed by fire do not experience significant live stemwood consumption, the entirety of the live stemwood biomass pool that is killed is transferred to the snag pool. Note that the field data and disturbance modelling

**Table 4.** Coarse Woody debris consumption rates from pre/post measurements in experimental fires

Ecozone	Low	Mod	High
BSW	0.024	0.163	0.140
TP	0.000	0.218	0.238
TSW	0.000	0.218	0.238
BP	0.359	0.509	0.412
BC	0.024	0.163	0.140
BSE	0.080	0.131	0.182
TSE	0.080	0.131	0.182
MC	0.024	0.163	0.140
HP	0.080	0.131	0.182
TC	0.024	0.163	0.140
PM	0.024	0.163	0.140
AM	0.080	0.131	0.182
MP	0.080	0.131	0.182
P	0.359	0.509	0.412

**Table 5.** Softwood fractional mortality by ecozone, as derived from median values from field studies

Ecozone	Low	Mod	High
BSW	0.45	0.81	1.00
TP	0.45	0.81	1.00
TSW	0.10	0.81	1.00
BP	0.45	0.81	1.00
BC	0.24	0.65	0.98
BSE	0.45	0.81	1.00
TSE	0.10	0.81	1.00
MC	0.28	0.74	0.98
HP	0.45	0.81	1.00
TC	0.24	0.65	0.98
PM	0.13	0.38	0.97
AM	0.28	0.34	0.95
MP	0.28	0.34	0.95
P	0.45	0.81	1.00

**Table 6.** Softwood crown fraction burned by ecozone, as derived from median values from field studies

Ecozone	Low	Mod	High
BSW	0.0	0.81	1.00
TP	0.0	0.81	1.00
TSW	0.1	0.81	1.00
BP	0.0	0.81	1.00
BC	0.0	0.65	0.98
BSE	0.0	0.81	1.00
TSE	0.1	0.81	1.00
MC	0.0	0.74	1.00
HP	0.0	0.81	1.00
TC	0.0	0.65	1.00
PM	0.0	0.38	0.97
AM	0.0	0.34	0.95
MP	0.0	0.34	0.95
P	0.0	0.81	1.00

160 undertaken here only accounts for tree mortality within the calendar year of the fire, and delayed mortality of over one year has been documented in boreal low and moderate severity fires (Angers et al., 2011) where less than half of total mortality occurs after the year of the fire. Thus, the modelling here does not account for delayed mortality that may extend upwards of 5 years after fire.

165 Crown Fraction Burned (CFB) speaks to the fraction of the live canopy that is itself consumed in the flaming front. The alternate outcomes being survival of the foliage, or the mortality of the tree without canopy consumption, resulting in the dropping of foliage onto the forest floor. From the axioms stated earlier, the CFB must be lower than or equal to the mortality rate, using field studies that show any partial crown consumption is likely sufficient to result in high rates if not complete mortality (Hood and Lutes, 2017), which is the case in Canada's trees with primarily thin bark. Due to the structure of the CBM, all High Severity fires have their mortality in the merchantable and smaller trees set to exactly 1.0, which is no more than a 5% variance from observed values. From field studies, the following ecozone-specific CFB values are found:

The consumption of live bark biomass is a pool in the model, and consumption rates can be defined by severity class. At the moment, lacking robust field data on bark biomass consumption rates across ecozones and severity classes (which are a small portion of the overall biomass), the bark proportional consumption rate is set to 34% of the overstory mortality rate, based only on a single set well-observed high severity fires in the Taiga Plains by [santín2015].

175 A major distinction is made between softwood and hardwood trees, where in Canada's boreal forests, a large fraction of hardwood trees (see Appendix E) are able to resprout even when the main stem has been killed by an intense forest fire (Brown

**Table 7.** Ecozone-level average fraction of hardwood overstory species that do not suffer extensive belowground biomass mortality after fire

Ecozone	Resprout Fraction
BSW	0.75
TP	0.75
TSW	0.94
BP	0.99
BC	0.76
BSE	0.67
TSE	0.78
MC	0.97
HP	0.80
TC	0.27
PM	0.39
AM	0.76
MP	0.32
P	0.99

and DeByle, 1987). Accordingly, the root mortality rates differ greatly between softwoods and hardwoods, with softwood root mortality equal precisely to stem mortality, while in resprouting hardwoods, little root mortality is observed even after intense fire (Pérez-Izquierdo et al., 2019). Though GCBM can resolve a species list down to the pixel level, currently an ecozone-level regional average composition of hardwood species with resprouting traits is used and is shown below:

Concurrently, the fraction of fine roots contained within the combustible forest floor layers can be a close to or exceeding 50% of the fine root biomass (Strong and La Roi, 1985), and burns alongside the organic soils (Benscoter et al., 2011). As a result, the calculation for softwood fine root consumption and mortality are as follows, using Softwood as an example:

$$SWFineRootConsump = SW.Mort \times SW.Prop.Fine.Root.duff \times Duff.Consump.Fract \quad (5)$$

$$SWFineRootMort.AG = SW.Mort \times SW.Prop.Fine.Root.duff \times (1 - Duff.Consump.Fract) \times (1 - ReSproutFactor) SWFineRootConsump \quad (6)$$

In contrast, the larger diameter of the coarse root biomass pool prevents its consumption during any smouldering of the duff layer, and the mortality rate of coarse roots is simply proportional to that of the stemwood overall.

## **2.8.2 Understory tree mortality and consumption**

Understory (or small diameter overstory) tree mortality is defined separately in the model, but given the lack of data on diameter  
190 classes in the severity data, robust field data on differing mortality rates of smaller diameter trees is not available, and so the  
understory tree mortality rate is set equal to the overstory rate as defined in the table above. Note that trees with a top height  
less than 1.4 m are not considered in this pool, and instead are lumped into the “other” pool.

## **2.8.3 Snag and stump consumption**

Compared to live stemwood of the same diameter, the low moisture content of standing dead stemwood (snags) allows for  
195 much greater consumption during the passage of an intense flaming front. The snag branch pool experiences almost complete  
combustion, while the largest biomass pool of the main standing dead stemwood

## **2.9 Construction fire disturbance matrices**

Give total number of global parameters, and parameters per ecozone, and then total parameters, and what % of total parameters  
we have so far filled with data

## **200 2.10 Calculation of Annual Direct C Emissions from Fire**

To compute an estimate of the total direct C emissions from forest fires in Canada in 2023, the classified burn severity product  
from the National Burned Area Composite annual production was utilized (see Hall et al 2020 for an algorithm description). In  
NBAC, an internal tracking value “NFIREID” is utilized, which is the final satellite-derived burned area polygon (allowing for  
multi-part polygons) is split across any RU unit boundaries (if any). Since carbon pool sizes vary across RU boundaries, this  
205 allows for a single NFIREID to be present across multiple RUs.

A total of 2199 fires as small as 0.09 ha (one 30x30 landsat pixel) were mapped by NBAC for burn severity for a total of  
14.60 Mha, but only fires over 100 ha were utilized as a lower limit of where meaningful per-fire estimates of the fraction of  
low, moderate, and high severity burned area was available. Including only fires 100 ha and larger reduced the total number of  
fires to 966 but the total area remained largely the same at 14.58 Mha. A total of 189,704 ha of post-fire salvage logging was  
210 also mapped in 2023 and is assigned to the moderate severity class after consultation with provincial land managers. The direct  
C emissions from fire shown here are not altered by the act of post-fire salvage logging. Additionally, the NBAC mapping  
process accounts for unburned islands (and areas with a mapped fire severity no different than unburned) which count towards  
the total fire area but do not have a disturbance matrix and direct C estimate applied.

A unique DM was then calculated for each fire using the median area-weighted Drought Code per fire. All thermal detection  
215 hotspots from VIIRS that intersect a fire were extracted from the historical hotspot archive that supports the Canadian smoke  
emissions model CFFEPPS-FireWork (Chen et al., 2019). The median DC value across all intersecting hotspots was used to  
derive a single DM per fire, no matter the duration of burning (could show first and last hotspot as a figure?).

To compute total direct fire emissions per fire, a single estimate of the carbon pool size based on the Reconciliation Unit of the centroid of the NFIREID polygon was applied. Since polygons are split across RU boundaries, the spatial weighting of  
220 the pool size per fire is performed automatically. While spatially explicit biomass maps are available for some aboveground components (SCANFI) and some belowground components (Hanes), the majority of the required pool sizes in CBM for the computation of the fire DMs are available only at the spatially referenced RU scale.

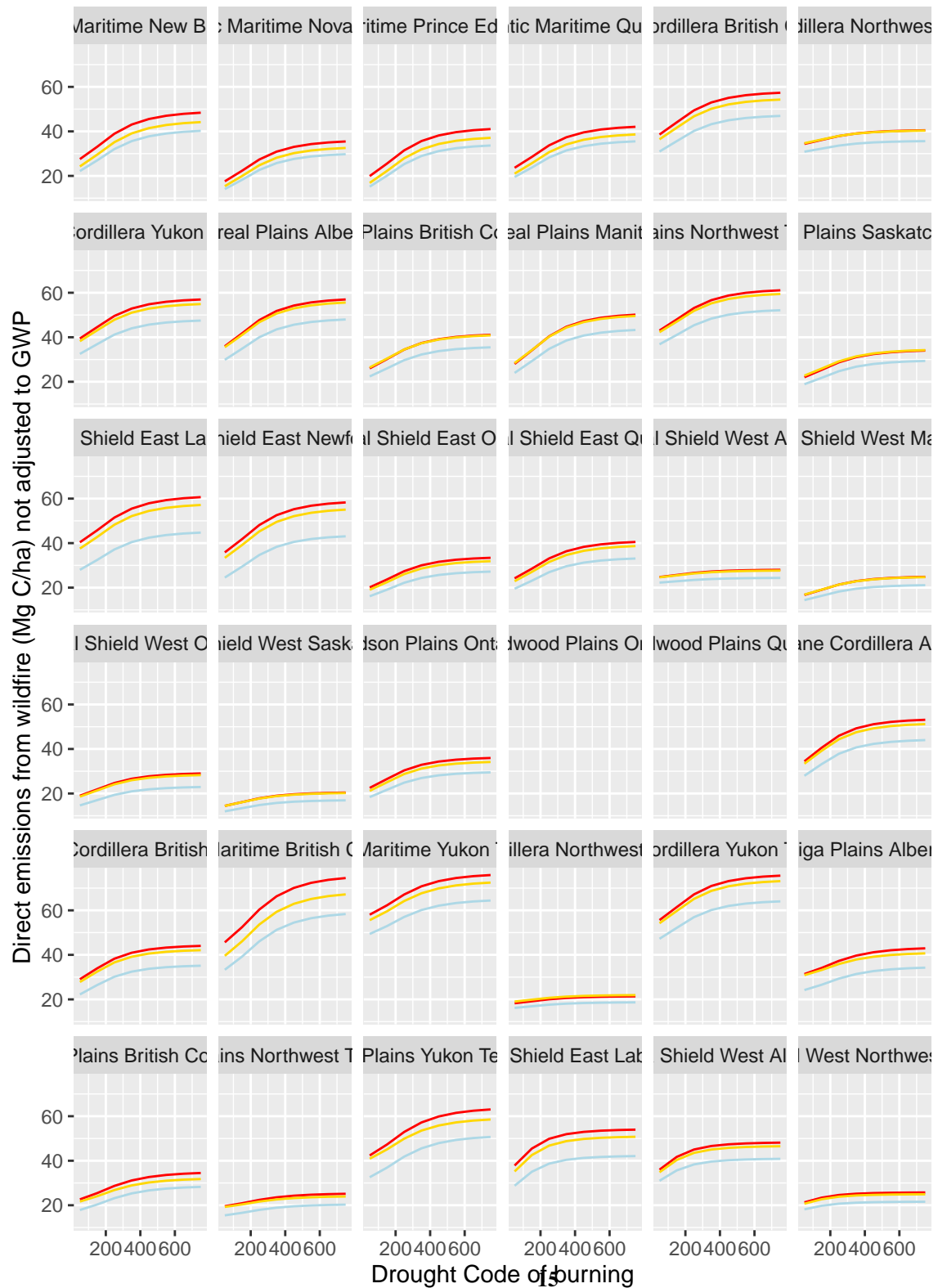
### 3 Results and Discussion

**Table 8.** High severity Disturbance Matrix in BP

	Softwood Merchantable	Softwood Stem Snag	Medium DOM	Softwood Foliage	Aboveground Very Fast DOM	CO2	CH4	CO	PM25
Softwood Merchantable	0	1							
Softwood Stem Snag		0	0.90000			0.0868000	0.0005000	0.0070000	0.0019000
Medium DOM			0.57624			0.2979033	0.0055089	0.0682254	0.0169504
Softwood Foliage				0	0.00	0.8680000	0.0050000	0.0700000	0.0190000
Aboveground Very Fast DOM					0.02	0.8506400	0.0049000	0.0686000	0.0186200
CO2									
CH4									
CO									
PM25									



### 3.1 Direct fire carbon emissions as a function of fire severity and drought



## 3.2 Comparison against observed direct fire emissions

### 3.2.1 Plot-level comparisons

Experimental fires at the International Crown Fire Modelling Experiment (Stocks et al., YYYY) provides a good example of detailed pre- and post-fire biomass measurements in pools that largely mirror the pools impacted by direct fire emissions modelled here. The series of burns in the Taiga Plains ecozone of the Northwest Territories were conducted under a median Drought Code of 363. The average Total Fuel Consumption (TFC) across the high severity crown fire burns was 4.2 kg/m<sup>2</sup> of biomass consumption, accounting for foliage, branchwood, woody debris, and forest floor consumption. The corresponding estimate using the fire Disturbance Matrices constructed here predicts 4.7 kg/m<sup>2</sup> of TFC, or 23.7 t C/ha. Across the nine ICFME fires, 62% of fuel consumption measured on-site was at the surface (forest floor plus woody debris). The model schema estimates that 80% of the fuel consumption was at the surface, suggesting a bias towards larger litter and duff pool size or higher surface fuel consumption in the model compared to this single site.

[function call to delete later] EmissionsPerFire(ID="ICFME\_avg",Area\_ha = 1,EcoBoundaryName="Taiga Plains",AdminBoundaryName="Northwest Territories",Low\_frac=0.0,Mod\_frac=0.0,High\_frac=1.0,Median\_DC=363) []

Experimental fires in the Boreal Shield East of Ontario showed mixed results when comparing well-observed biomass consumption in wildfires to model outputs. Three high severity crown fires in mature Jack pine stands at Kenshoe Lake at an average Drought Code of 129 (see de Groot et al 2022) were observed to have 2.87 kg/m<sup>2</sup> average Total Fuel Consumption, as compared to model estimates of 4.56. In part this is due to lower surface fuel consumption: the model output estimated 75% of TFC to be derived from surface fuel consumption, while measured surface fuel consumption was only 40% of TFC. Future iterations of this fire DM scheme that incorporate site-specific surface fuel loadings (Hanes et al duff map AB) will improve model representations of fuel consumption in locations with fuel loadings that substantially deviate from the average pool sizes used in this iteration of the model.

[function call to delete later] EmissionsPerFire(ID="Kenshoe Lake passive crown fires 5 9 12",Area\_ha = 1,EcoBoundaryName="Boreal Shield East",AdminBoundaryName="Ontario",Low\_frac=0.0,Mod\_frac=0.0,High\_frac=1.0,Median\_DC=((65+145+178)/3)) []

Also in the Boreal shield East of Ontario, six high severity crown fires in immature (~30 year old) Jack Pine under slightly higher Drought Code conditions (average DC 232) showed higher observed average surface fuel consumption (1.9 kg/m<sup>2</sup>) owing to more woody debris. Total fuel consumption observed at Sharpsands was 3.0 kg/m<sup>2</sup>, as compared to modelled consumption of 5.3 kg/m<sup>2</sup> (26.8 t C/ha); the observed surface contribution to total fuel consumption of 64% was broadly similar to the modelled value of 75%. Again, given the regional fixed biomass pool sizes used, it would be expected that the model overestimates total fire emissions in younger stands.

[function call to delete later] EmissionsPerFire(ID="Sharpsands 11-17",Area\_ha = 1,EcoBoundaryName="Boreal Shield East",AdminBoundaryName="Ontario",Low\_frac=0.0,Mod\_frac=0.0,High\_frac=1.0,Median\_DC=232) []

In the Taiga Plains of Alberta, continuous crown experimental fires in black spruce forest at Big Fish lake burned at an average Drought Code of 241 were observed to consume 1.65 kg/m<sup>2</sup> in the surface and 0.86 kg/m<sup>2</sup> of biomass in the canopy.

**Table 9.** Comparison of the Modified Combustion Efficiency (MCE) of airborne gas measurements of Canadian wildfires against modelled MCE

Study	Date	Subset	Ecozone	Drought Code	Obs MCE	Modelled MCE
Hornbrook et al 2011	2008-07-01	Afternoon (0.2Low 0.4Mod 0.4High)	Boreal Shield West	250	0.92	0.908
Hornbrook et al 2011	2008-07-01	Late Evening (100% low severity)	Boreal Shield West	250	0.82	0.903
Hornbrook et al 2011	2008-07-04	After rain smouldering only low severity	Boreal Shield West	275	0.83	0.903

260 Similar to the Boreal Shield East examples, observed fuel consumption was lower than the model output of 7.4 kg/m<sup>2</sup>, owing to a high bias in modelled canopy fuel consumption (1.85 kg/m<sup>2</sup>) as well as surface fuel consumption (model value of 5.5 kg/m<sup>2</sup>), though the modelled contribution of surface fuel consumption to the total of 74% is comparable to the 66% surface fuel contribution in the observation data.

265 [function call to delete later] EmissionsPerFire(ID=“Big Fish Active Crown only”,Area\_ha = 1,EcoBoundaryName=“Taiga Plains”,AdminBoundaryName=“Alberta”,Low\_frac=0.0,Mod\_frac=0.0,High\_frac=1.0,Median\_DC=241) []

270 Overall, the plot-level comparisons of this model to experimental fires showed a high model bias in the estimation of the surface fuel consumption in the Ontario and Alberta examples with lower Drought Codes. Although site-specific calibration of absolute fuel consumption rates is possible, the current iteration of the fire DMs still relies on fixed biomass pools per RU, so an honest performance assessment of the model was made against these regional biomass values even when more detailed site-specific biomass pool data is available for each experimental fire.

275 A further comparison can be made in the contribution of surface fuels to total fuel consumption, which partially accounts for site-specific differences in absolute biomass pool size (e.g. foliage biomass otherwise known as Crown Fuel Load in experimental fires). In all cases except Kenshoe Lake, the bias in the modelled contribution of surface fuels in the model was 10-20% higher than the observed contribution of surface fuels which was 62-66% outside of Kenshoe Lake where surface fuels were only 40% of total fuel consumption.

245 !!! Then some discussion here (or at the start of this) on duff consumption patterns from the ecology literature? <https://cdnsciencepub.com>

### 3.2.2 Forest fire observations of CO and CO<sub>2</sub> emissions ratios

280 Hornbrook et al (2011) reported the mean observed Modified Combustion Efficiency for distinct periods during the ARCTAS campaign over northern Saskatchewan in 2008. MCE observed by aircraft during the peak burn period when the majority of fuel consumption and area burned occurs (0.92) largely corresponded with modelled values (0.91), suggesting the model provides a fair representation of the balance of flaming and smouldering during large active wildfires. Subsequent smoke plume observations during periods of greatly reduced spread and intensity (late evening and after rain) showed a substantially reduced MCE of 0.82-0.83 that indicates a near lack of flaming combustion. Even when represented as 100% low severity fire in the 285 model, the modelled MCE only declines to 0.903. Since the fire DM model is based on area burned, fire activity such as

smouldering but with minimal actual area burned increased is going to show an MCE far lower than areas of low severity fire spread, which are typically still a low subcanopy flaming front that features a mix of smouldering duff and woody debris alongside flaming consumption of litter (McRae et al., 1994; McRae et al., 2017).

### 3.3 2023 Canadian wildfire season total direct emissions

290 A total of 471 Mt C was estimated to be released directly by fires in Canada in 2023. The total mass of PM2.5 emissions was estimated as  $3.1248862 \times 10^7$  Mt of total mass, assuming a 50% carbon content. [[(need to break this down more as a table by P/T or RU? can also do median DC and median total C/ha by RU). As a map?]]. The area-weighted mean Drought Code for all fires in Canada in 2023 was 444, representing moderate but not exceptional drought conditions in Canada's northern forests. The area-weighted mean total C emissions per unit area was 32.3, though 90% of the emissions per unit area were between the 295 5th percentile of 13 t C/ha typical of the Taiga Plains ecozone under low Drought Code conditions and the 95th percentile of 13 t C/ha typical of Pacific coastal forests.

Byrne et al 2024 used observed total atmospheric column excess CO and a range of MCE values to estimate total fire C emissions in Canada in 2023 of between 570-727 Mt C with a mean estimate of 647 Mt. The uncertainty in the estimate from Byrne et al 2024 lies primarily in the uncertain CO<sub>2</sub>:CO ratio (more commonly computed as the normalized ratio MCE).  
300 Our bottom-up estimates that partition flaming vs smouldering shows a lower CO<sub>2</sub>:CO estimate of 5.79. This lower CO<sub>2</sub>:CO ratio (i.e. more smouldering) if applied to the data from Byrne et al 2024 would reduce their lower range of total C emissions to 486.78 Mt C, which is comparable to the 471 Mt C computed from this bottom-up approach. Estimates of total carbon emissions based solely on the sum of observed Fire Radiative Power (FRP) from Copernicus-CAMS was approximately 490 Mt C (<https://atmosphere.copernicus.eu/smoke-canadian-wildfires-reaches-europe>)

305 -some other discussion points (unordered) so far

- given the generic nature of these DMs and their simple relative simplicity, can be added to other frameworks like LANDIS (see Stenzel 2019 as well, they do some of that).
- paragraph on extended impacts like delayed stem mortality, rapid snag fall, and changes (or not) in duff decomposition rates. Not (as of yet) covered in this 1-timestep pulse disturbance described here.

310 -future work on biomass maps in GCBM will improve this emissions estimates only marginally, since during large fire years with drought such as 2023 there is little fuel selection bias in burned area.

- paragraph on extended impacts like delayed stem mortality, rapid snag fall, and changes (or not) in duff decomposition rates. Not (as of yet) covered in this 1-timestep pulse disturbance described here.

-future work on biomass maps in GCBM will improve this emissions estimates only marginally, since during large fire years with drought such as 2023 there is little fuel selection bias in burned area. # Conclusions

The conclusion goes here.

#### 4 Appendix A: list of fluxes and corresponding fire-related plain-language summary.

#### 5 Appendix B: non-linear least squares modelling of soil organic layer consumption

For national annual estimates of forest organic soil layer consumption during wildfire, implementations that only utilize  
320 Canadian experimental fire data from the Fire Behaviour Prediction System will be limited to a maximum consumption value of 5 kg/m<sup>2</sup> of total surface fuel (woody debris, litter, and duff) of 5 kg/m<sup>2</sup>, or 25 Mg C/ha, given the observation dataset and fitted model parameters. For the common C-2 Boreal Spruce fuel type for instance, Surface Fuel Consumption (kg m<sup>2</sup>) is modelled as:

$$SFC = 5.0 \left(1 - e^{-0.0115 BUI}\right)^{1.0} \quad (7)$$

325 This model form has the distinct advantage of SFC being 0.0 at a BUI of zero. The model parameters vary by fuel type (i.e. deciduous broadleaf fuels are limited to 1.5 kg/m<sup>2</sup> of maximum SFC) but are fixed within a fuel type.

More recent observations and modelling from de Groot et al. (2009) extended the FBP data with an additional 128 observations from 7 additional wildfires, and the ABoVE project compiled over 1000 field observations of depth of burn and C stocks before and after wildfire in Canada and Alaska, over 600 of which are in North American Level II ecoregions also occurring in Canada  
330 (fix Walker 2020 ORNL DAAC ref in bibtex here). de Groot et al. (2009) provides a concise and informative improvement on the FBP fuel consumption equations, where both a Fire Weather Index System component (in this case, Drought Code) is used similarly to Buildup Index in the FBP, but importantly, the site-level organic soil layer fuel load is also accounted for, which allows for the greater absolute combustion in deeper organic soils that is moderated by the natural logarithm transformation:

$$\log_e(FFFC) = -4.252 + 0.710\log_e(DC) + 0.671\log_e(FFFL) \quad (8)$$

335 where FFFC is Forest Floor Fuel Consumption (SFC minus surface woody debris) in kg m<sup>2</sup> and FFFL is Forest Floor Fuel Load in kg/m<sup>2</sup>. This model fits well within the dataset and extends the observed maximum FFFC to nearly 10 kg/m<sup>2</sup>. The ABoVE synthesis of FFFL and FFFC (Walker et al 2020 ORNL) expands upon a slightly smaller dataset used in a modelling summary also by Walker et al (2020 NCC), where structural equation modelling was used to explore drivers of FFFC but no concise and readily reproducible modelling is produced. The results of the SEM from Walker et al (2020 NCC) emphasized a  
340 greater role of FFFL over DC, though coarse reanalysis that lacked local fire agency weather stations was used. An analysis of just 2014 fires in the Northwest Territories by (walker2018) showed that while the mean depth of burn across all black spruce stands was 6-10 cm, the driest (xeric) black spruce stands with the smallest FFFL showed upwards of 75% soil organic consumption, while deeper organic soils in subhygric black spruce stands showed less than 25% consumption.

To provide the largest possible dataset for FFFC and FFFL, the ABoVE synthesis was combined with wildfire data from  
345 de Groot et al 2009 not otherwise found in the ABoVE synthesis. The ABoVE synthesis sites in the Alaska Boreal Interior ecoregion, which have equivalent Canadian ecozone were excluded, but Alaska Boreal Cordillera sites near the Yukon border

were utilized. Experimental fire data from the FBP data was not used, as deeper combustion measurements resulting from hours and days of smouldering combustion captured in wildfire data are not available in experimental fires where extensive smouldering is not measured due to suppression. In order to best represent on-the-ground Fire Weather Index values, the  
 350 Drought Code and other FWI values from Walker et al 2020 reanalysis were substituted with interpolated weather station (both Environment and Climate Change Canada as well fire agency stations). This data also has the benefit of being properly overwintered for Drought Code (Hanes DC overwinter) and capturing small rain events not captured in reanalysis that meaningfully impact the Duff Moisture Code in particular.

For the purposes of improving national estimates of the fractional soil organic layer loss during wildfire, this framework  
 355 emphasizes the proportional C stock loss (as with all CBM disturbance matrices) rather than the absolute value of combustion. In contrast to the modelling of absolute combustion value, any analysis of proportions is best conducted as logit- transformed data, where the logit transformation is:

$$\text{logit}(p) = \log \frac{p}{1 - p} \quad (9)$$

which effectively transforms a data of proportions of [0,1] to a Gaussian distribution with a range of approximately -5 to +5  
 360 (in this dataset), and a mode approximately at zero. Within the logit-transformed data, exploratory analysis of ecozones as a factor alongside other non-linear splines of FWI values and FFFL was conducted:

```

## 
## Family: gaussian
## Link function: identity
365 ##
## Formula:
## prop_sol_combusted_logit ~ s(drought_code, k = 4, bs = "tp") +
##     ecozone + s(BGslow.Mg.C.ha, k = 4, bs = "tp")
##
370 ## Parametric coefficients:
##                 Estimate Std. Error t value Pr(>|t|)
## (Intercept)  0.11939   0.09318   1.281  0.2005
## ecozoneBP   -0.29433   0.15506  -1.898  0.0581 .
## ecozoneBSW  -0.19928   0.15988  -1.246  0.2131
375 ## ecozoneTP   -0.23049   0.11476  -2.008  0.0450 *
## ecozoneTSW  -0.29887   0.12157  -2.458  0.0142 *
## ---
## Signif. codes:  0 '***' 0.001 '**' 0.01 '*' 0.05 '.' 0.1 ' ' 1
## 
```

```

380 ## Approximate significance of smooth terms:
##                                edf Ref.df      F p-value
## s(drought_code)    1.352  1.618  2.862  0.0631 .
## s(BGSlow.Mg.C.ha) 2.950  2.998 232.720 <2e-16 ***
## ---
## Signif. codes:  0 '***' 0.001 '**' 0.01 '*' 0.05 '.' 0.1 ' ' 1
##
## R-sq. (adj) =  0.628  Deviance explained = 63.3%
## -REML = 869.04  Scale est. = 0.81207 n = 651

```

(could also show boxplots?) which shows that the Boreal Cordillera ecozone has a meaningfully higher proportional soil organic layer consumption rate compared to BP, BSW, TP, and TSW, all of which are not significantly different in consumption rates once DC and FFFC (shown as BGSlow.Mg.C.ha) are accounted for. Boreal Cordillera data were set aside for a distinct model.

Similar to de Groot et al. (2009), Drought Code was a better predictor of consumption rates than Buildup Index as used in the FBP. In the logit transformed space, saturation-type non-linear curve using the relevant FWI component was fitted in a non-linear least squares model, but an additive term of the natural-logarithm transformed FFFC (given as BGSlow pool in Mg C/ha) was used as well. In the end, a superior model was found using the proportional depth of burn, rather than the proportional loss of the mass of the soil organic layer. The non-linear least squares model fit was conducted using the Levenberg-Marquardt nonlinear least-squares algorithm found in MINPACK (Elzhov et al 2023) R package, which supported bounded parameter constraints.

In the abstract, the model follows the form:

$$\text{logit} \left( \frac{\text{depthofburn}}{\text{pre-fireorganicdepth}} \right) = [c(1 - e^{(aDC)})] + (b \log_e(\text{BGSlow})) \quad (10)$$

with fitted parameters as:

$$\text{logit} \left( \frac{\text{depthofburn}}{\text{pre-fireorganicdepth}} \right) = [3.83(1 - e^{(-0.005DC)})] + (-0.718 \log_e(\text{BGSlow})) \quad (11)$$

Note the “b” coefficient on the parameter associated with the FFFL (BGSlow) of -0.718, which results in larger organic layer fuel loads leading to smaller proportional consumption values, which follows the patterns shown by Walker 2018 for NWT fires of 2014.

The a parameter term that forms the exponent of e alongside Drought Code is related to the DC value at which half of the maximum possible asymptotic consumption value is observed (for a given FFFL value). The NLS fitting was given a minimum value of -0.06 such that half of the asymptotic maximum consumption rate was modelled as occurring at or around a DC value of 300. The other parameters were fit to the best possible value with no constraint.

Importantly, since fire behaviour, emissions modelling, and carbon accounting all operate with the calculation of mass loss and depth of burn, a correction factor was applied that corrects for the trends in bulk density with depth for C-2 fuels as given by de Groot et al. (2009), so that a model of proportional depth of burn is then converted into a proportional mass loss term:

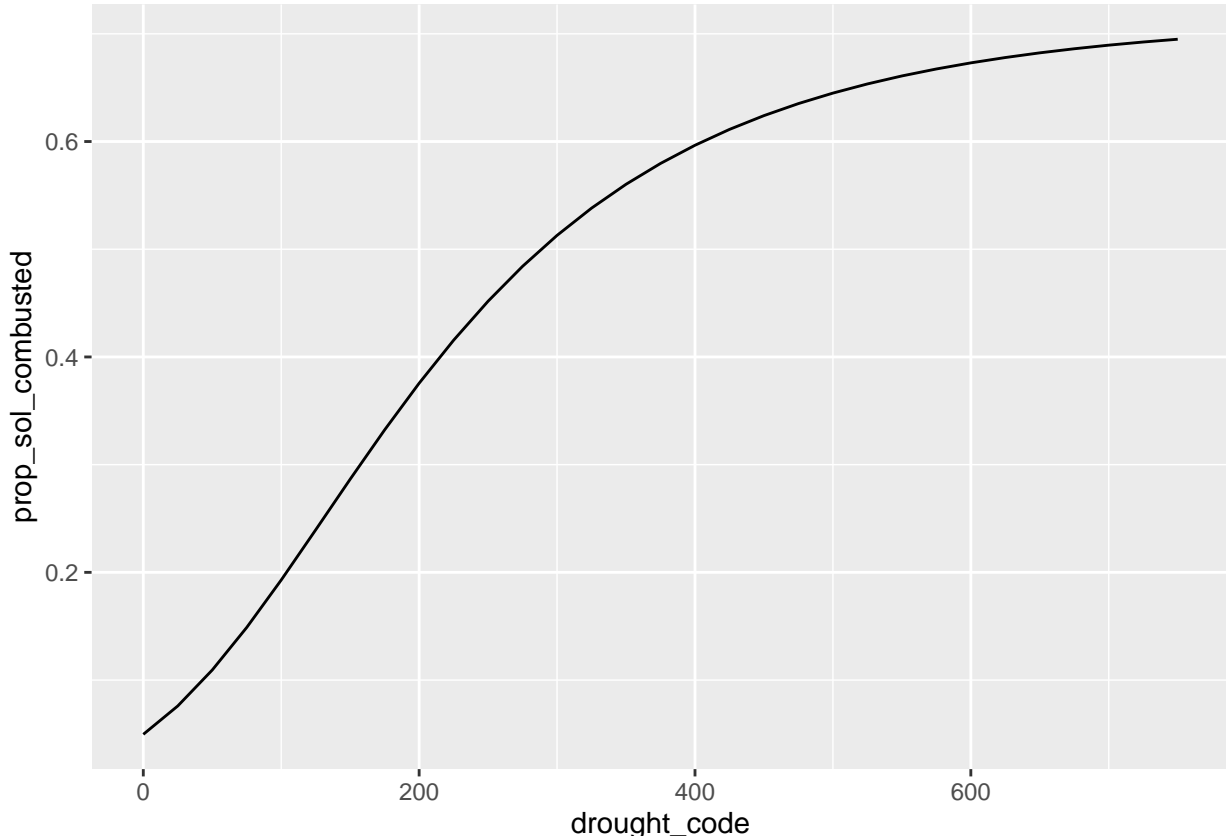
$$\left( \frac{FFFC}{FFFL} \right) = 1.017 \left( \frac{\text{depthofburn}}{\text{pre-fireorganicdepth}} \right)^{0.250} \quad (12)$$

415 which for example means that the median proportional depth of burn in the AboVE/de Groot training data of 0.40 corresponds to 0.32 of the proportional mass loss (since shallow organic soil is less dense), or a correction factor of 0.80. For non-spruce-dominated fuels, this correction is much smaller but still meaningful:

$$\left( \frac{FFFC}{FFFL} \right) = 0.13 \left( \frac{\text{depthofburn}}{\text{pre-fireorganicdepth}} \right) + 0.87 \quad (13)$$

420 (show perhaps what a few different a values look like?) (also compute the DC value of about half the maximum FBP SFC values too, just for kicks)

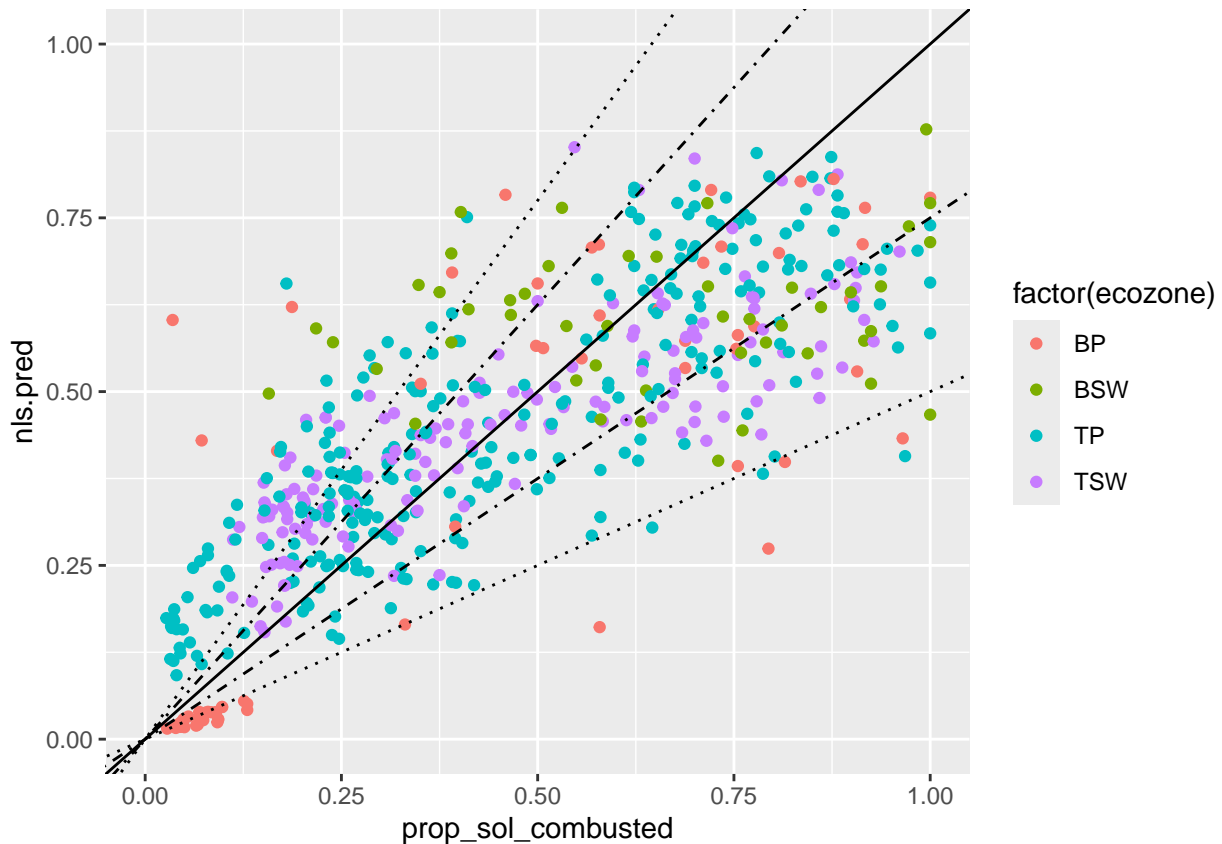
For example, using a moderately thick ~12 cm thick organic soil layer, the proportion of consumption as a function of Drought Code using the model above



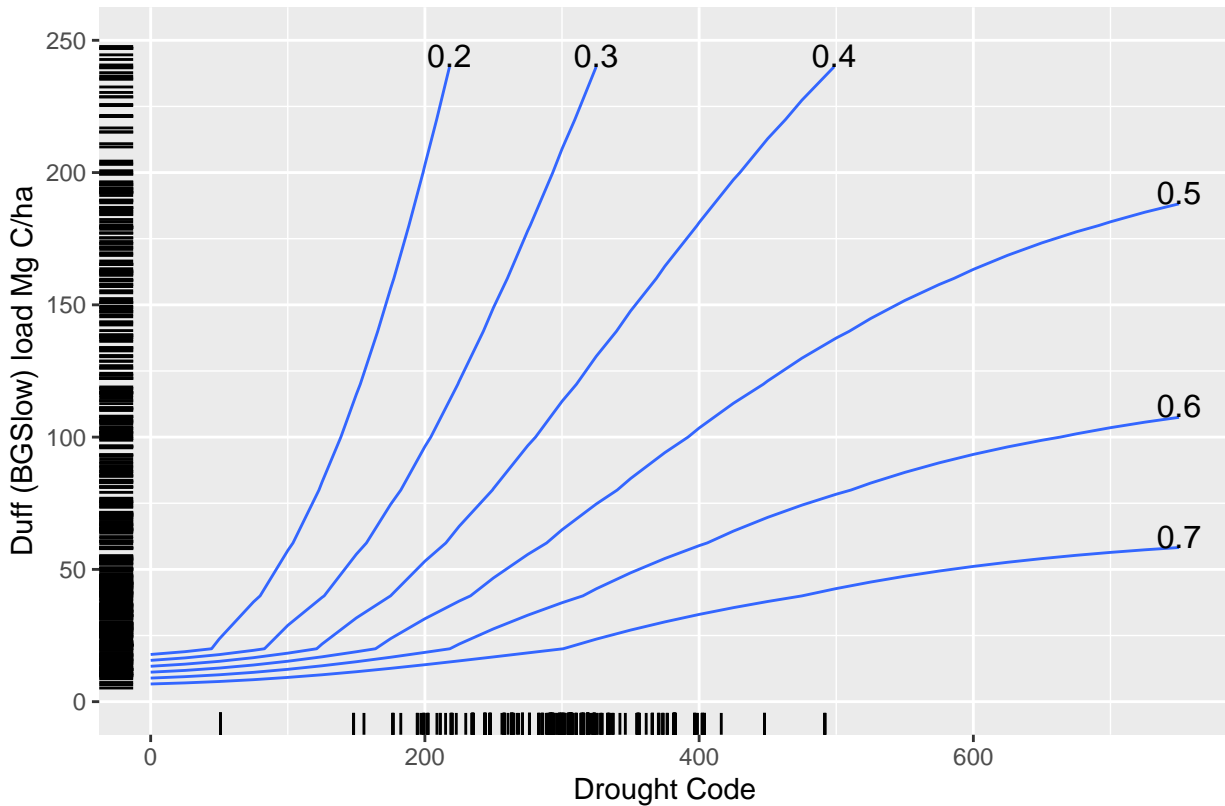
With the parameter constrained NLS fitting, the proportional consumption model for the forest floor has a leave-one-out

425 (conducted at the fire-level, not plot) cross validated r2 of ###, and a Mean Percent Error of ###%

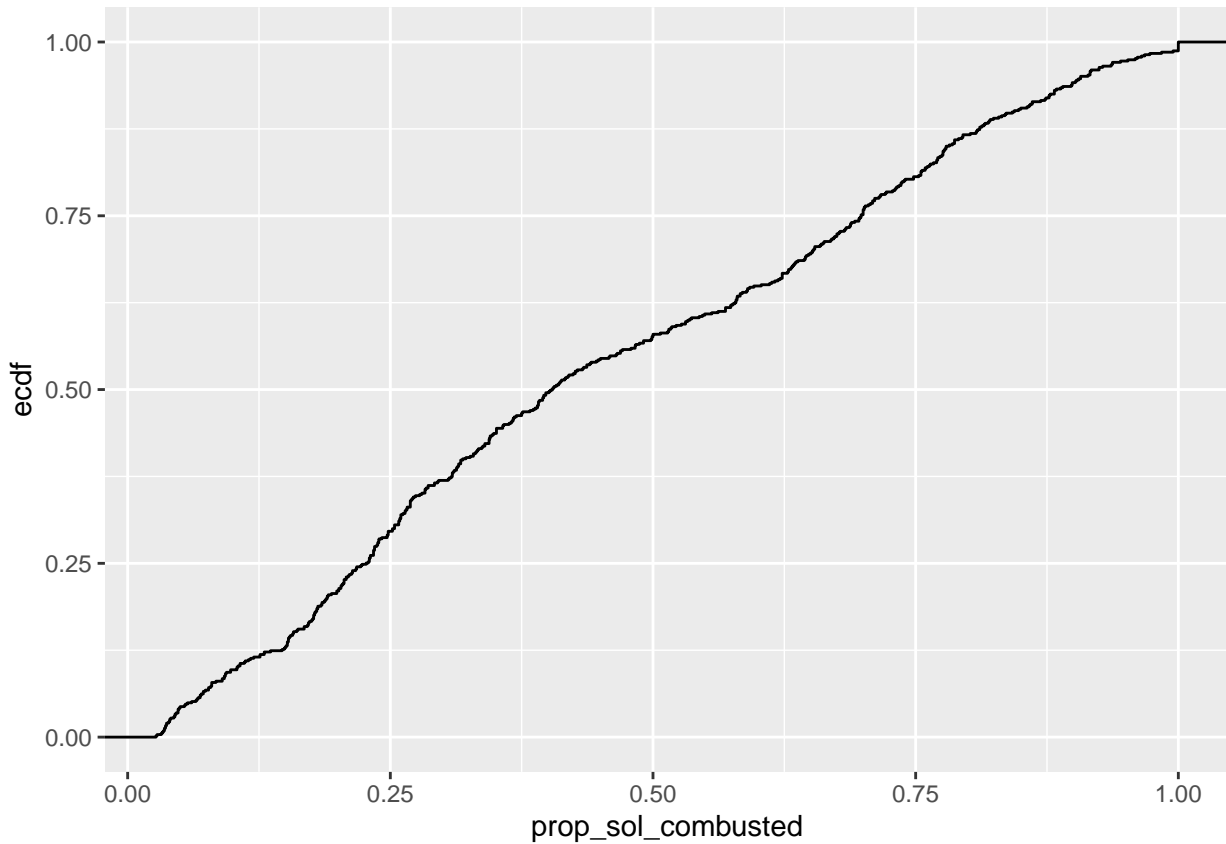
```
## Scale for y is already present.  
## Adding another scale for y, which will replace the existing scale.  
## Scale for y is already present.  
## Adding another scale for y, which will replace the existing scale.  
430 ## Scale for x is already present.  
## Adding another scale for x, which will replace the existing scale.
```



Across the entire parameter space of Drought Code and BGSlow pool size, the following isolines of proportional consumption in the model can be plotted:



Isoline contours of equal organic soil layer consumption fraction as a function of Drought Code and the organ



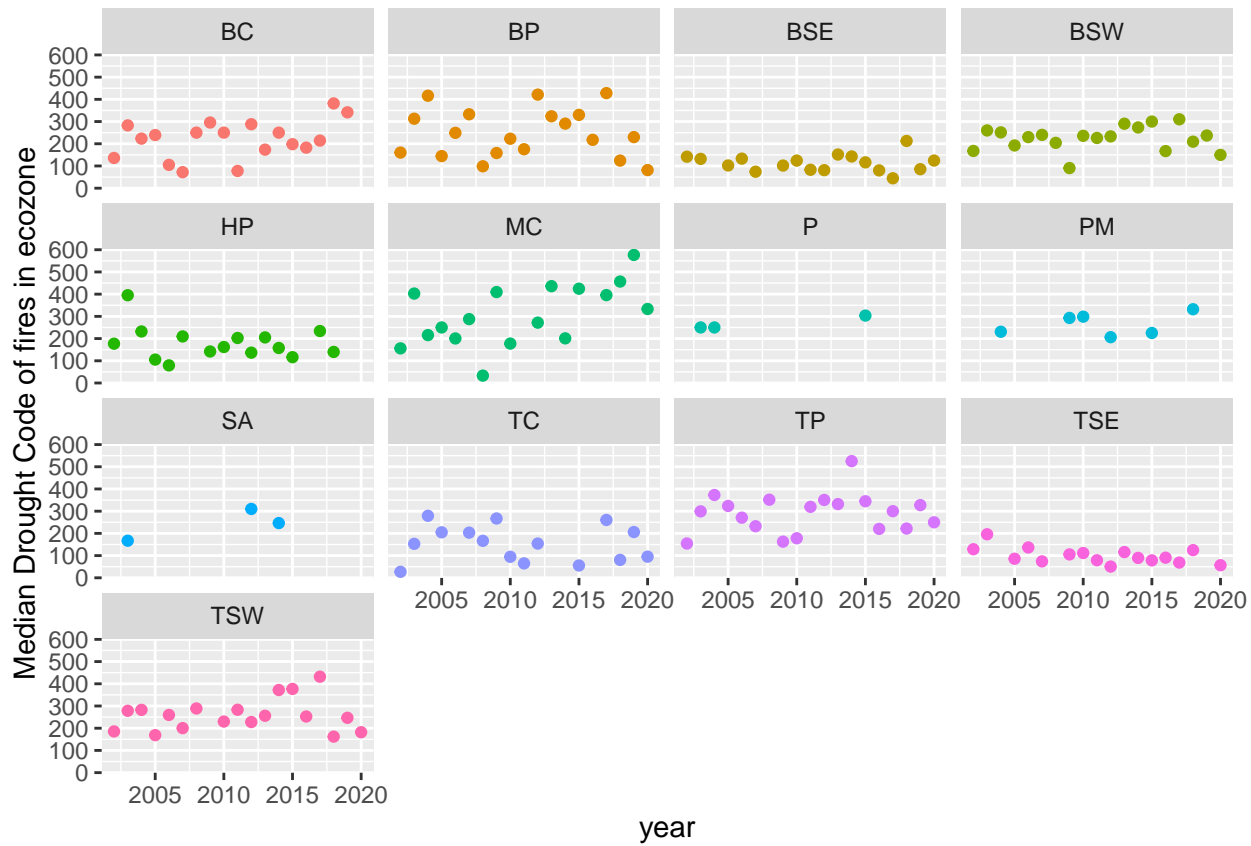
### 5.0.1 Boreal Cordillera modelling

For the Boreal Cordillera, a simple linear model on the logit-transformed data was found to be the best performing model for estimating soil organic consumption proportion:

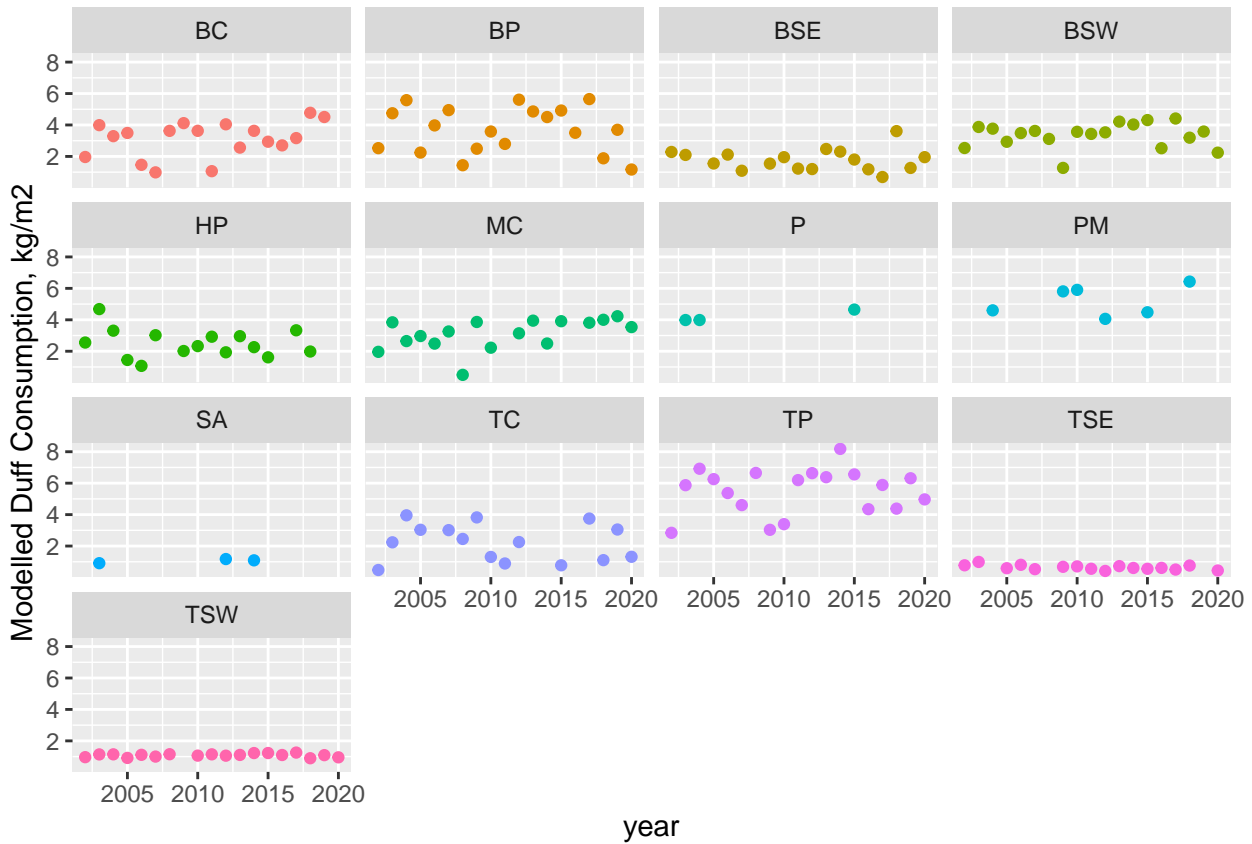
$$440 \quad \text{logit} \left( \frac{FFFC}{FFFL} \right) = (0.00257 * DC) + (-0.54 * \log_e(BGSlow)) + 2.17 \quad (14)$$

Despite the presence of a fixed intercept term, the strong inverse dependence on the natural logarithm of the BGSlow pool size (FFFL) results in zero proportional consumption when Drought Code is equal to zero.

## 6 Appendix C: annual variability in observed Drought Code during wildfire spread, and impact on ecozone-level average forest floor emissions



445



## 7 Appendix D: Representative photos

Photos of: (1) partial litter consumption; (2) partial vs full duff consumption; (3) mortality but not consumption of understory trees with live overstory; (4) mortality but not consumption of overstory trees; (5) mixedwood severity example showing 450 consumption of broadleaf foliage; (6) woody debris consumption; (7) snag preferential consumption relative to little to no bole consumption in live trees

Give lat/long, year, ecozone, severity class, and leading spp for each photo, maybe other relevant metrics? From some of the experimental fires mostly??

## 8 Appendix E: List of Resprouting Hardwoods of Canada

455 Alnus spp. Arbutus men. Betula all. Betula pap. Betula pop. Fraxinus ame. Fraxinus nig. Fraxinus pen. Populus bal. Populus gra. Populus tre. Populus tri. Quercus spp. Salix spp.

## Appendix A: List of fluxes and corresponding fire-related plain-language summary

### A1 Option 1

460 If you sorted all figures and tables into the sections of the text, please also sort the appendix figures and appendix tables into the respective appendix sections. They will be correctly named automatically.

### A2 Option 2

If you put all figures after the reference list, please insert appendix tables and figures after the normal tables and figures.

\appendixfigures needs to be added in front of appendix figures \appendixtables needs to be added in front of  
465 appendix tables

Please add \clearpage between each table and/or figure. Further guidelines on figures and tables can be found below. Regarding figures and tables in appendices, the following two options are possible depending on your general handling of figures and tables in the manuscript environment: To rename them correctly to A1, A2, etc., please add the following commands in front of them:

470 . Thompson and Whitman contributed to the concept and code design with the assistance of Hanes, Hudson

. The authors declare no competing interests.

. The algorithm and results presented only apply to boreal and temperate forest ecosystems where sufficient ground plots of fire severity are available. As a data-driven model, this framework is not suitable for other ecosystems nor agricultural or forestry biomass burning practices.

. Thanks to (insert names here)

475 **References**

- Angers, V. A., Gauthier, S., Drapeau, P., Jayen, K., Bergeron, Y., Angers, V. A., Gauthier, S., Drapeau, P., Jayen, K., and Bergeron, Y.: Tree mortality and snag dynamics in North American boreal tree species after a wildfire: a long-term study, *International Journal of Wildland Fire*, 20, 751–763, <https://doi.org/10.1071/WF10010>, publisher: CSIRO PUBLISHING, 2011.
- Barber, Q. E., Jain, P., Whitman, E., Thompson, D., Guindon, L., Parks, S. A., Wang, X., Hethcoat, M., and Parisien, M.: The Canadian Fire Spread Dataset, <https://doi.org/10.17605/OSF.IO/F48RY>.
- Benscoter, B. W., Thompson, D. K., Waddington, J. M., Flannigan, M. D., Wotton, B. M., Groot, W. J. d., and Turetsky, M. R.: Interactive effects of vegetation, soil moisture and bulk density on depth of burning of thick organic soils, *International Journal of Wildland Fire*, 20, 418–429, <https://doi.org/10.1071/WF08183>, 2011.
- Bernier, P. Y., Gauthier, S., Jean, P.-O., Manka, F., Boulanger, Y., Beaudoin, A., and Guindon, L.: Mapping Local Effects of Forest Properties on Fire Risk across Canada, *Forests*, 7, 157, <https://doi.org/10.3390/f7080157>, 2016.
- Bona, K. A., Shaw, C., Thompson, D. K., Hararuk, O., Webster, K., Zhang, G., Voicu, M., and Kurz, W. A.: The Canadian model for peatlands (CaMP): A peatland carbon model for national greenhouse gas reporting, *Ecological Modelling*, 431, 109 164, <https://doi.org/10.1016/j.ecolmodel.2020.109164>, 2020.
- Brown, J. K. and DeByle, N. V.: Fire damage, mortality, and suckering in aspen, *Canadian Journal of Forest Research*, 17, 1100–1109, <https://doi.org/10.1139/x87-168>, publisher: NRC Research Press, 1987.
- Chen, J., Anderson, K., Pavlovic, R., Moran, M. D., Englefield, P., Thompson, D. K., Munoz-Alpizar, R., and Landry, H.: The FireWork v2.0 air quality forecast system with biomass burning emissions from the Canadian Forest Fire Emissions Prediction System v2.03, *Geoscientific Model Development*, 12, 3283–3310, <https://doi.org/10.5194/gmd-12-3283-2019>, 2019.
- de Groot, W., Pritchard, J., and Lynham, T.: Forest floor fuel consumption and carbon emissions in Canadian boreal forest fires, *Canadian Journal of Forest Research*, 39, 367–382, <https://doi.org/10.1139/X08-192>, 2009.
- Group, F. C. F. D. R.: Development and structure of the Canadian Forest Fire Behavior Prediction System, vol. ST-X-3, Forestry Canada, <https://cfs.nrcan.gc.ca/publications?id=10068>, 1992.
- Hall, R. J., Freeburn, J. T., Groot, W. J. d., Pritchard, J. M., Lynham, T. J., Landry, R., Hall, R. J., Freeburn, J. T., Groot, W. J. d., Pritchard, J. M., and et al.: Remote sensing of burn severity: experience from western Canada boreal fires, *International Journal of Wildland Fire*, 17, 476–489, <https://doi.org/10.1071/WF08013>, 2008.
- Hall, R. J., Skakun, R. S., Metsaranta, J. M., Landry, R., Fraser, R. H., Raymond, D., Gartrell, M., Decker, V., and Little, J.: Generating annual estimates of forest fire disturbance in Canada: the National Burned Area Composite, *International Journal of Wildland Fire*, <https://doi.org/10.1071/WF19201>, 2020.
- Hanes, C. C., Wang, X., Jain, P., Parisien, M.-A., Little, J. M., and Flannigan, M. D.: Fire-regime changes in Canada over the last half century, *Canadian Journal of Forest Research*, 49, 256–269, <https://doi.org/10.1139/cjfr-2018-0293>, 2019.
- Hanes, C. C., Wang, X., Groot, W. J. d., Hanes, C. C., Wang, X., and Groot, W. J. d.: Dead and down woody debris fuel loads in Canadian forests, *International Journal of Wildland Fire*, 30, 871–885, <https://doi.org/10.1071/WF21023>, publisher: CSIRO PUBLISHING, 2021.
- Hayden, K., Li, S.-M., Liggio, J., Wheeler, M., Wentzell, J., Leithead, A., Brickell, P., Mittermeier, R., Oldham, Z., Mihele, C., Staebler, R., Moussa, S., Darlington, A., Steffen, A., Wolde, M., Thompson, D., Chen, J., Griffin, D., Eckert, E., Ditto, J., He, M., and Gentner, D.: Reconciling the total carbon budget for boreal forest wildfire emissions using airborne observations, *Atmospheric Chemistry and Physics Discussions*, pp. 1–62, <https://doi.org/10.5194/acp-2022-245>, publisher: Copernicus GmbH, 2022.

- Hessburg, P. F., Miller, C. L., Parks, S. A., Povak, N. A., Taylor, A. H., Higuera, P. E., Prichard, S. J., North, M. P., Collins, B. M., Hurteau, M. D., Larson, A. J., Allen, C. D., Stephens, S. L., Rivera-Huerta, H., Stevens-Rumann, C. S., Daniels, L. D., Gedalof, Z., Gray, R. W., Kane, V. R., Churchill, D. J., Hagmann, R. K., Spies, T. A., Cansler, C. A., Belote, R. T., Veblen, T. T., Battaglia, M. A., Hoffman, C., Skinner, C. N., Safford, H. D., and Salter, R. B.: Climate, Environment, and Disturbance History Govern Resilience of Western North American Forests, *Frontiers in Ecology and Evolution*, 7, <https://doi.org/10.3389/fevo.2019.00239>, 2019.
- Hood, S. and Lutes, D.: Predicting Post-Fire Tree Mortality for 12 Western US Conifers Using the First Order Fire Effects Model (FOFEM), *Fire Ecology*, 13, 66–84, <https://doi.org/10.4996/fireecology.130290243>, 2017.
- Jain, P., Barber, Q. E., Taylor, S. W., Whitman, E., Castellanos Acuna, D., Boulanger, Y., Chavardès, R. D., Chen, J., Englefield, P., Flannigan, M., and et al.: Drivers and Impacts of the Record-Breaking 2023 Wildfire Season in Canada, *Nature Communications*, 15, 6764, <https://doi.org/10.1038/s41467-024-51154-7>, 2024.
- Kurz, W. A., Apps, M., Banfield, E., and Stinson, G.: Forest carbon accounting at the operational scale, *The Forestry Chronicle*, 78, 672–679, <https://doi.org/10.5558/tfc78672-5>, 2002.
- Letang, D. and de Groot, W.: Forest floor depths and fuel loads in upland Canadian forests, *Canadian Journal of Forest Research*, 42, 1551–1565, <https://doi.org/10.1139/x2012-093>, 2012.
- 525 McAlpine, R. S.: Testing the Effect of Fuel Consumption on Fire Spread Rate, *International Journal of Wildland Fire*, 5, 143–152, <https://doi.org/10.1071/wf9950143>, 1995.
- Michaletz, S. T. and Johnson, E. A.: A heat transfer model of crown scorch in forest fires, *Canadian Journal of Forest Research*, 36, 2839–2851, <https://doi.org/10.1139/x06-158>, publisher: NRC Research Press, 2006.
- 530 Parisien, M.-A., Barber, Q. E., Hirsch, K. G., Stockdale, C. A., Erni, S., Wang, X., Arseneault, D., and Parks, S. A.: Fire deficit increases wildfire risk for many communities in the Canadian boreal forest, *Nature Communications*, 11, 1–9, <https://doi.org/10.1038/s41467-020-15961-y>, 2020.
- Pérez-Izquierdo, L., Clemmensen, K. E., Strengbom, J., Nilsson, M.-C., and Lindahl, B.: Quantification of tree fine roots by real-time PCR, *Plant and Soil*, 440, 593–600, <https://doi.org/10.1007/s11104-019-04096-9>, 2019.
- 535 Simon, H., Beck, L., Bhave, P. V., Divita, F., Hsu, Y., Luecken, D., Mobley, J. D., Pouliot, G. A., Reff, A., Sarwar, G., and Strum, M.: The development and uses of EPA's SPECIATE database, *Atmospheric Pollution Research*, 1, 196–206, <https://doi.org/10.5094/APR.2010.026>, 2010.
- Simpson, I. J., Akagi, S. K., Barletta, B., Blake, N. J., Choi, Y., Diskin, G. S., Fried, A., Fuelberg, H. E., Meinardi, S., Rowland, F. S., Vay, S. A., Weinheimer, A. J., Wennberg, P. O., Wiebring, P., Wisthaler, A., Yang, M., Yokelson, R. J., and Blake, D. R.: Boreal forest fire emissions in fresh Canadian smoke plumes: C<sub>1</sub>-C<sub>10</sub> volatile organic compounds (VOCs), CO<sub>2</sub>, CO, NO<sub>2</sub>, NO, HCN and CH<sub>3</sub>CN, *Atmospheric Chemistry and Physics*, 11, 6445–6463, <https://doi.org/10.5194/acp-11-6445-2011>, publisher: Copernicus GmbH, 2011.
- 540 Skakun, R., Castilla, G., Metsaranta, J., Whitman, E., Rodrigue, S., Little, J., Groenewegen, K., and Coyle, M.: Extending the National Burned Area Composite Time Series of Wildfires in Canada, *Remote Sensing*, 14, 3050, <https://doi.org/10.3390/rs14133050>, 2022.
- Stinson, G., Thandi, G., Aitkin, D., Bailey, C., Boyd, J., Colley, M., Fraser, C., Gelhorn, L., Groenewegen, K., Hogg, A., and et al.: A new approach for mapping forest management areas in Canada, *The Forestry Chronicle*, 95, 101–112, <https://doi.org/10.5558/tfc2019-017>, 2019.
- Stocks, B. J., Mason, J. A., Todd, J. B., Bosch, E. M., Wotton, B. M., Amiro, B. D., Flannigan, M. D., Hirsch, K. G., Logan, K. A., Martell, D. L., and et al.: Large forest fires in Canada, 1959–1997, *Journal of Geophysical Research: Atmospheres*, p. FFR 5–12, <https://doi.org/10.1029/2001JD000484>, 2002.

- 550 Strong, W. L. and La Roi, G. H.: Root density-soil relationships in selected boreal forests of central Alberta, Canada, *Forest Ecology and Management*, 12, 233–251, [https://doi.org/10.1016/0378-1127\(85\)90093-3](https://doi.org/10.1016/0378-1127(85)90093-3), 1985.
- White, J. C., Wulder, M. A., Hermosilla, T., Coops, N. C., and Hobart, G. W.: A nationwide annual characterization of 25 years of forest disturbance and recovery for Canada using Landsat time series, *Remote Sensing of Environment*, 194, 303–321, <https://doi.org/10.1016/j.rse.2017.03.035>, 2017.
- 555 Whitman, E., Parisien, M.-A., Thompson, D. K., Hall, R. J., Skakun, R. S., and Flannigan, M. D.: Variability and drivers of burn severity in the northwestern Canadian boreal forest, *Ecosphere*, 9, e02128, <https://doi.org/10.1002/ecs2.2128>, 2018.
- Whitman, E., Parisien, M.-A., Holsinger, L. M., Park, J., and Parks, S. A.: A method for creating a burn severity atlas: an example from Alberta, Canada, *International Journal of Wildland Fire*, <https://doi.org/10.1071/WF19177>, 2020.